2.1 Materials Synthesis and Cell Fabrication

Overview

To understand the functioning of the battery and for better safety and design, in-depth knowledge of the characterization of electrode material is needed. In the present research work, I put much effort into developing a family of positive electrode materials for NIBs (Sodium-ion batteries). The primary motto revolves around synthesis, structural design and electrochemical performance of the cell with safety priority. The current instrumentation chapter deals with experimental and instrumentation methodology used for the validation of experimental results. The experimental technique includes structural, morphological, electronic, and electrochemical validation till material synthesis to the actual cell performance characterization. A short description of the instruments used in the experimental process and related terminology is mentioned.

This chapter consists of two sections:

(i) Synthesis process used for pristine electrode material and used cell fabrication methodology.

(ii) Characterization method used for structural, thermal, morphological, electrochemical analysis and corresponding data analysis.

2.1.1 Synthesis Methodology

Two methods of nanomaterial synthesis involve the Bottom-up and Top-down methods(Uddin et al., 2017). The top-down approach involves the reduction in size from bulk to nanoparticles, such as ball milling and sputtering, etc. (Y. Meng et al., 2016). The bottom-up process is the size building of nanomaterials from an atom by

atom or molecule by molecule(Pang et al., 2013). In the bottom-up process, chemical synthesis methods have many benefits, including the ability to create uniform nanomaterial size, shape, and distribution. Selecting the right process is crucial for creating great nanostructures. Polyanion-based architectures can be engineered through various synthetic methods like the hydrothermal method(Huang et al., 2005), sol-gel method(Cai et al., 2022), microwave-synthesis method (S. Liu et al., 2020), and coprecipitation method(X. Chen et al., 2022). Among these methods, the coprecipitation approach is effective for the fabrication of network material. Additionally, precipitation is a procedure that further removes soluble chemicals from the solution, making it an efficient way to create nanostructures. Furthermore, Aqueous solvents are used easily to prepare, and immediate product formation (within a short period), and uniform reaction within the species are the added merits of the coprecipitation methodology. The solution precipitation method involves the nucleation of a new phase and the growth of that phase. First is the nucleation, which arises when the concentration of precipitation embryo reaches the critical radius. Second is the growth of nuclei by the diffusion of two or more embryos or nuclei.

2.1.1.1 Coprecipitation Technique

It is the most facile synthesis technique, cost-effective, fast, and can apply to large-scale industrial processes. Eco-friendly synthesis route where no hazardous solvent is required(X. Chen et al., 2022; Cruz et al., 2018). Here precursor is taken in salt form and dissolved in deionized water in appropriate stoichiometric proportion. Cationic and Anionic salt is dissolved in a separate beaker and added dropwise on stirring condition, yielding to precipitate. The precipitate is filtered and grinded. Fine powder in then calcined as per the required temperature in the furnace, followed by the proper grinding

of the calcined powder. This obtained powder is further carried out for the further characterization process. The process chart of this technique is shown in figure 2.1

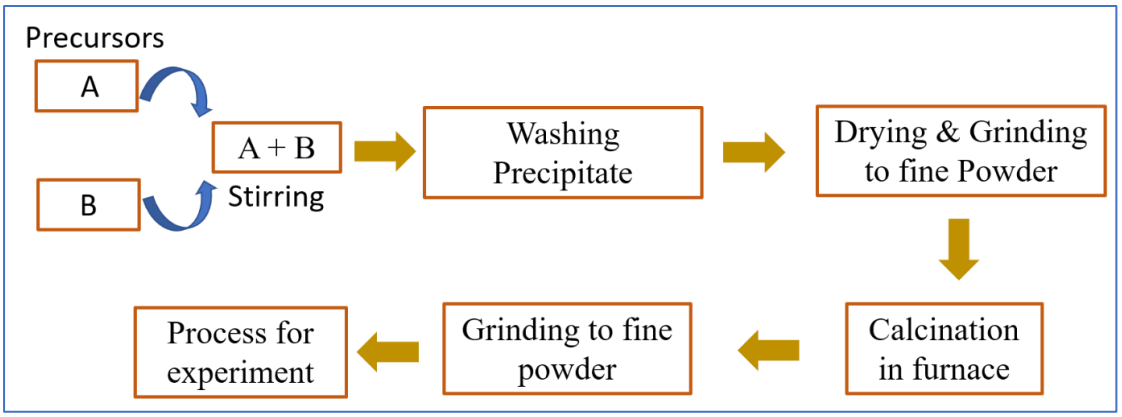

Figure 2.1 Synthesis steps of Coprecipitation technique.

2.1.2 Cell Fabrication

2.1.2.1 Slurry preparation

The initial active ingredients are combined to create an electrode slurry. The raw active ingredients are mixed with a solvent, binder, and additives to create an electrode slurry. The initial stage in making an electrode is slurry mixing, done separately for the anode and cathode. The major factor that affects the battery performance, quality and the electrode's uniformity are viscosity, density, and solid content(Ouyang et al., 2020). The way raw components are formulated, the processes involved in mixing, and the amount of time involved in mixing are all crucial factors. Dry mixing of active ingredients and conductive carbon in a solvent may reduce the slurry's viscosity, allowing for higher solid content and quicker drying at the expense of rate capability. Contrarily, incorporating binder into the slurry (active material and conductive carbon in solvent) provides a porous conductive framework(M. Wang et al., 2020). Beginning with the dry mixing of active ingredients and due Agglomerations are unavoidable

because of interactions (electrostatic forces, van der Waals attractions and hydrogen bonds) between slurry particles. Therefore, a dispersant must always be added throughout the mixing process.

2.1.2.2 Slurry Coating

Electrode slurry is applied to the current collector uniformly. Slot-die coating is the well establish coating process used for the industrial application capable of coating 300ft/min. The typical drying process involves three steps of solvent evaporation, binder diffusion, and particle sedimentation simultaneously. The safety and cycle life of the manufactured battery is significantly impacted by the quality of the coating and drying. Poor electrochemical performance of the battery and safety issues will emerge from material non-uniformity or defects introduced on the electrodes. The thickness of the Coating and mass loading should be controlled to minimize or avoid foil tearing and failure during the coating(Hawley Oak Ridge TN (United States); Univ. of Tennessee Knoxville TN (United States)] & Li Oak Ridge TN (United States); Univ. of Tennessee Knoxville TN (United States)] (ORCID:0000000287109847), 2019).

2.1.2.3 Electrode Pressing

The slurry coating on the current collector metal foil should be compact to improve current density. Need consistent thickness to provide further dust and humidity control for the electrode. Calendaring provides compact and uniform thickness and improved humidity and dust control to the electrode. Calendaring controls the electrode material thickness, porosity, and tortuosity(Meyer et al., 2017). Increasing calendaring reduces

active layer thickness and increases the volumetric energy density and electrode tortuosity that affects electrochemical impedance.

2.1.3 Cell Assembling

Sodium-ion battery (NIB) is the assembly of the cathode (Positive electrode) composed of sodium-containing framework type of material and anode (Negative electrode) composed of intercalation type of compound or Hard carbon. This electrode is connected through the electronically insulating separator soaked in the electrolyte, which only allows ion movement through it. Non-aqueous electrolyte containing 1M $NaPF_6$ in EC: DC: PC(Ponrouch et al., 2015) is discussed in Tables 1.2 and 1.3. The whole cell is assembled in Ar filled glove box (O_2 < 1ppm, H_2O < 0.1ppm) (Figure 2.3 a). The figure below shows two types of commonly used assembly: Swagelok (Figure 2.2) and Coin cell CR2032 (Figure 2.3 b).

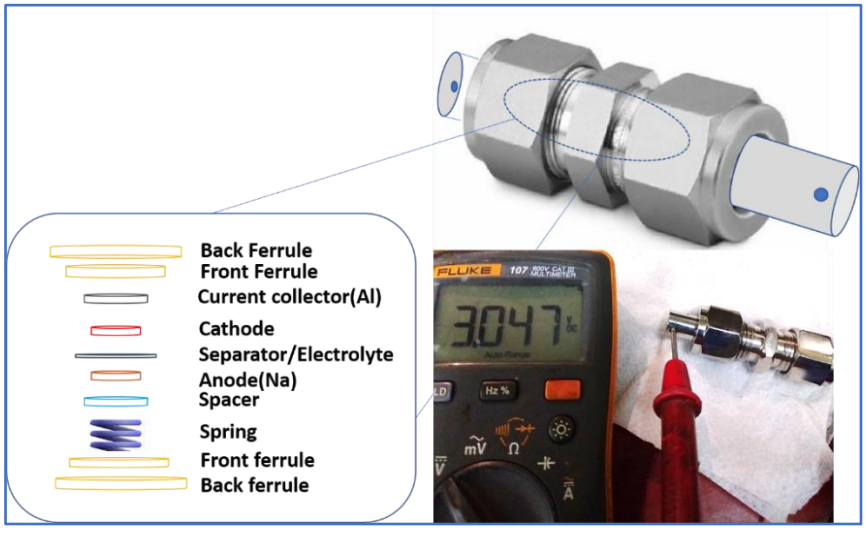

Figure 2.2: Schematic of Swagelok cell with the component.

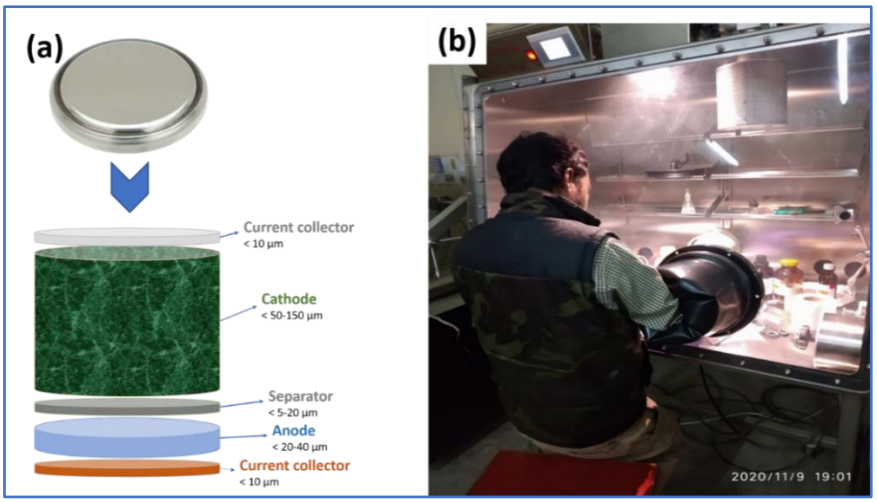

Figure 2.3: (a) Schematic of CR2032 coin cell component (b) Cell assembling in Glove Box (Dept of Ceramic Engg. IIT BHU Varanasi)

2.2 Physical and Electrochemical Characterization

Characterizations of material are broadly classified into two categories Physical and electrochemical. Firstly, Physical characterization is subdivided into structural, thermal, and morphological characterization. The structure of as-synthesized material is confirmed by X-Ray diffraction XRD (phase transition after intercalation/deintercalation of sodium is studied for better structural stability and safety point of view) (Lim et al., 2012; H. Yu et al., 2014), Fourier Transform Infrared Spectroscopy FTIR (as-synthesized material and prepared electrode clarify the functional changes on electrode) (Govindaraj & Mariappan, n.d.), X-ray Photon Spectroscopy XPS (determine chemical state of element) and Ultraviolet-Visible Spectroscopy UV-Vis. (electronic transition on photo response). The Thermogravimetric Analysis determines the temperature response of the material(Vijayan et al., 2011). Morphological analysis like particle shape, size, elemental composition and distribution of synthesized material and electrode is determined by SEM “Scanning Electron Microscopy” and EDS “Elemental Dispersive

Spectroscopy." The second is electrochemical characterization, where the electrochemical response of the material is studied. I will study this characterization in detail in the coming chapters.

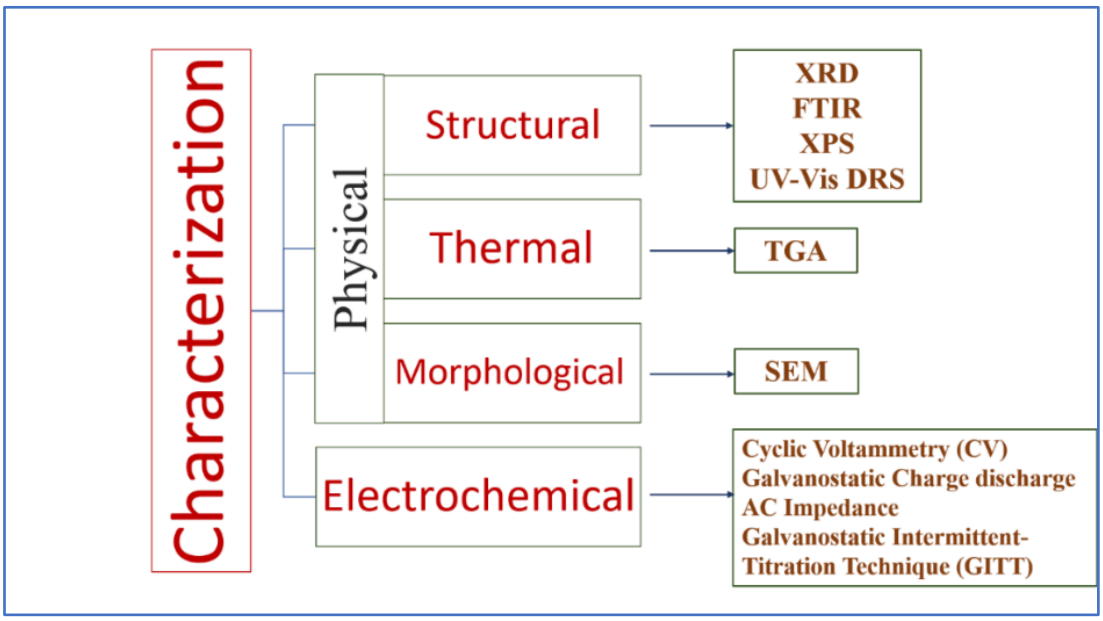

Figure 2.4 Schematic of characterization path for pristine powder and electrode.

2.2.1 Physical Characterization

2.2.1.1 X-Ray Diffraction (XRD)

XRD "X-ray Diffraction" is a powerful structural characterization tool used to identify the crystal structure and phase identification in crystalline materials. X-rays are scattered by each set of lattice planes at a unique angle, and the strength of the light scattered depends on the crystal's atomic configuration. The pattern of scattering from various plane sets is specific to the crystal structure of the particular substance. The X-ray tube produces X-rays by targeting a high-energy accelerated electron beam onto the Cu target. A monochromator is used to filter out the undesired photon. X-rays produced

in the wavelength of 10-0.01 nm are in order of lattice spacing and elastically diffracted through the atomic plane in the crystalline material. In my thesis work only, a powdered sample is used. The Structural characterization of materials like phase composition, grain size, preferred orientation, lattice strain, and defect structure is determined. Measurement is taken in the form of angle and diffracted beam intensity. Obtained raw data is refined and presented as a 3D crystal structure by determining the mean atomic position from the electron density from its atomic position(Jian et al., 2017b). The X-Ray beam is generated by bombarding the Cu target with an emitting electron from the hot filament. If the X-rays' wavelength is the same as the separations between the planes of the crystal structure, they can be reflected so that the angle of reflection and angle of incidence are equal. The XRD intensities can provide quantitative data that is exactly about the atomic configurations at interfaces. The powder sample mounted on the sample holder is inclined by angle θ while the detector rotates around it at angle 2θ. The diffraction phenomenon is described by the Braggs as follows:

$$2d \sin \theta = n\lambda \qquad \text{(Eq. 2.1)}$$

Where d represents the interplanar spacing, θ represents the angle of incidence and n is the integer, and λ is the wavelength of the incident beam. X-ray diffraction study is carried out on benchtop Rigaku Miniflex 600, as shown in Figure 2.5(a) and its diffraction phenomenon through the crystal is shown in the schematic of Figure 2.5 (b).

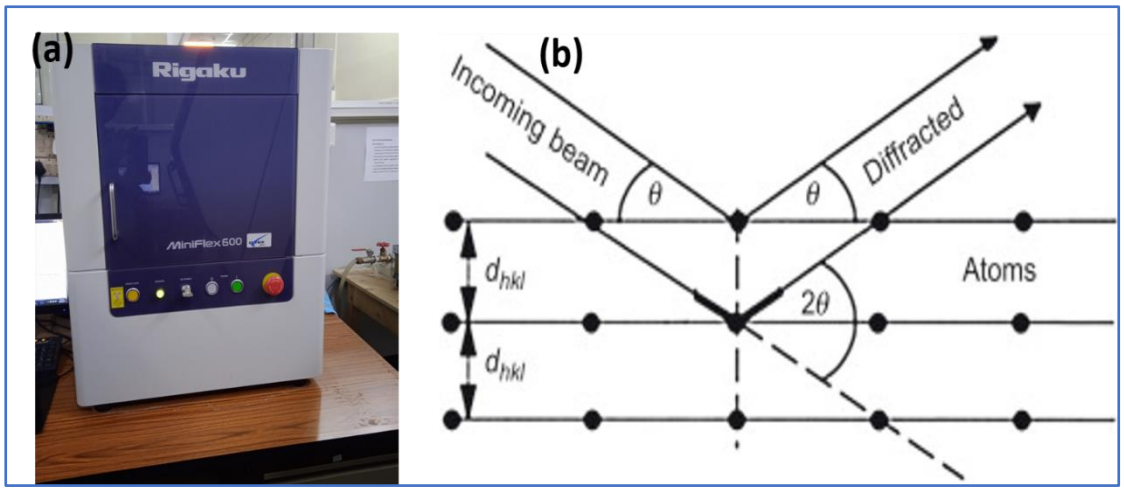

Figure 2.5 (a) Photograph of X-ray diffractometer (Courtesy: CIF IIT(BHU)) (b) Schematic of X-ray diffraction into the sample (Courtesy: Science Direct)

Crystallite size is also determined from the peak broadening by Deby- the shearer formula as follows

$$D = k \lambda / \beta \cos\theta \qquad \text{(Eq. 2.2)}$$

where D (crystallite size, nm), k (Shape factor of average crystallite, 0.9), β (FWHM, in radian), and θ (peak position, in radian), Cu Kα is 1.54 Å. The crystalline contribution of of material to the total is calculated using the following formula.

$$\% \text{ Crystallinity} = \text{Area of crystalline peak} / \text{Area of (Crystalline + Amorphous) peak.} \qquad \text{(Eq. 2.3)}$$

Thus, the most common application of X-ray powder diffraction is to identify unidentified crystalline materials. Additionally, Rietveld refinement allows XRD to evaluate sample purity, determine the crystal structure, and quantify the size of unit cells.

2.2.1.2 Fourier Transform Infrared (FTIR) Spectroscopy

infrared spectroscopy is based on how molecules' atoms vibrate. It is usual to practice generating an infrared spectrum by shining infrared light on a sample and counting how much of the incident light is absorbed at each energy level. Any peak in an absorption spectrum corresponds to the frequency of a particular sample molecule's component's vibration at the energy at which it appears. A molecule requires to have an electric dipole moment that must vary while it is vibrating in order to exhibit infrared absorption. This is the infrared spectroscopy selection rule. For a heteronuclear diatomic molecule that is "infrared-active." Such a molecule experiences a dipole moment change when the bond stretches and contracts. In contrast, a homonuclear diatomic molecule is an illustration of an "infrared-inactive" molecule since its dipole moment is zero regardless of how long the link is. It is possible to imagine a diatomic molecule as two vibrating masses joined by a spring. Atom bonded in the molecule is compared to a spring; anytime the spring is stretched or compressed past its equilibrium range, the system's potential energy rises. The amount of energy proportional to the frequency of vibration is(Pavia, 2015)

$$E = hv \qquad \text{(Eq. 2.4)}$$

For force constant K of the spring or its stiffness masses m_1 and m_2 of the two bonded atoms. the frequency of vibration of a bond is given by the equation

$$\nu = 1/2\pi c\sqrt{K/\mu} \qquad \text{(Eq. 2.5)}$$

is the Hooks law for vibrating spring, where μ is reduced mass and

$$\mu = (m_1 * m_2)/ (m_1 + m_2) \qquad \text{(Eq. 2.6)}$$

where K is the constant, which varies according to the bond. K for a strong bond is higher than for a weak bond. In my research work Nicolet iS5 model (made by Thermo Fisher) FTIR instrument is used in the range of 400 4000 cm^{-1}.

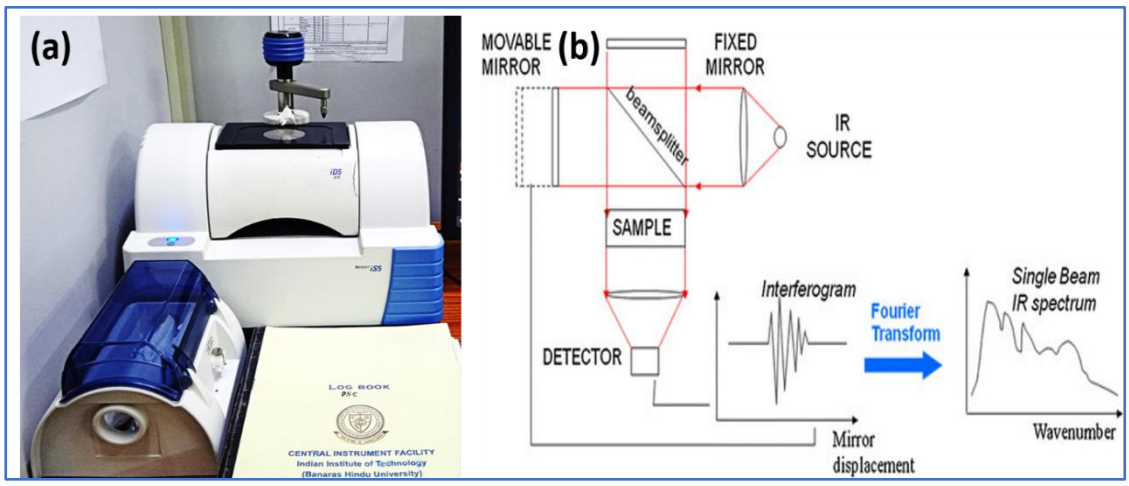

Figure 2.6 (a) Photograph of FTIR spectrophotometer instrument (Courtesy: CIF IIT(BHU)) (b) Schematic of conventional FTIR spectrophotometer (Courtesy: Research gate).

2.2.1.3 X-Ray Photoelectron Spectroscopy (XPS)

XPS "X-ray photoelectron spectroscopy" is used to study the surface chemistry of a material. Chemical information like % age of the element present, chemical state of an element, and binding energy of the electronic state. A narrow beam of X-ray is bombarded on the sample surface, and sample electrons absorb energy and emit it from the surface. These electrons are called photoelectrons. These photoelectrons are of low energy, and these come from a depth of nearly 10 nm. These electrons carry information on the chemical state of the element and the atomic information in the sample. The *KE* "kinetic energy" of the photoemitted electron is the difference between incident beam energy minus binding energy and the work function of the element. All XPS study is carried out on the XPS K-alpha model of Thermo Fisher XPS. The analyzer is kept in

a high-vacuum chamber with pressure below 10^{-8} bar. The XPS binding energy spectra were obtained in the fixed analyzer transmission mode at the pass energy of 20 eV.

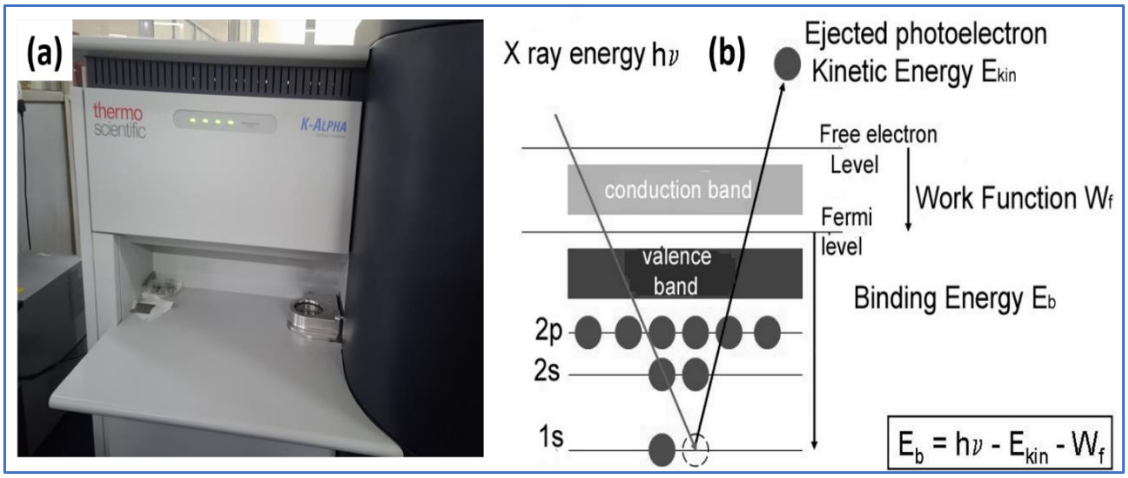

Figure 2.7 (a) Photograph of XPS instrument (Courtesy: CIF IIT (BHU)) (b) Schematic of XPS working principle.

2.2.1.4 UV-Visible Spectroscopy

Electronic transitions between electronic energy levels are what cause electromagnetic radiation to be absorbed in the UV-Vis part of the spectrum. An electron is moved from an occupied orbital to an unoccupied orbital with a higher potential energy as a molecule absorbs energy. The highest occupied molecular orbital (HOMO) to the lowest unoccupied molecular orbital (LUMO) transition is typically the most likely (LUMO). The electronic transition and optical band gap property of a material is studied using the UV-VIS-DRS method (Figure 2.8) in the wavelength range of 200-900 nm. It is convenient to measure the optical properties by the UV-VIS-DRS method, but for band gap calculation, reflectance or transmittance spectra cannot be used directly because of the low intensity of the Eg transition. Diffuse reflectance spectra are transformed into the Kubelka -Munk function *F(R)* vs. wavelength. Spectra recorded in

diffuse reflectance (R) transformed to absorption coefficient K and scattering coefficient S as per Kubelka Munk model(Makuła et al., 2018) [98].

$$\frac{K}{S} = \frac{(1-R)^{\wedge}2}{2R} \equiv F(R) \qquad \text{(Eq. 2.7)}$$

Tauc plot $$(\alpha h\nu)^{1/n} = A\,(h\nu - E_g) \qquad \text{(Eq. 2.8)}$$

is transformed by replacing absorption coefficient α with the Kebulka Munk function $F(R)$ as

$$(F(R)h\nu)^{1/n} = A\,(h\nu - E_g) \qquad \text{(Eq. 2.9)}$$

Where h = planks constant, *v* frequency of light, A is Absorbance, E_g is band gap of the material, and n = 1/2 (direct allowed transition), 2 (indirect allowed transition). The optical band gap was calculated from a Tauc plot of $(F(R)h\nu)^2$ vs. photon energy ($h\nu$). All UV experiments were done on Shimadzu 2600 UV Spectrophotometer in my thesis work

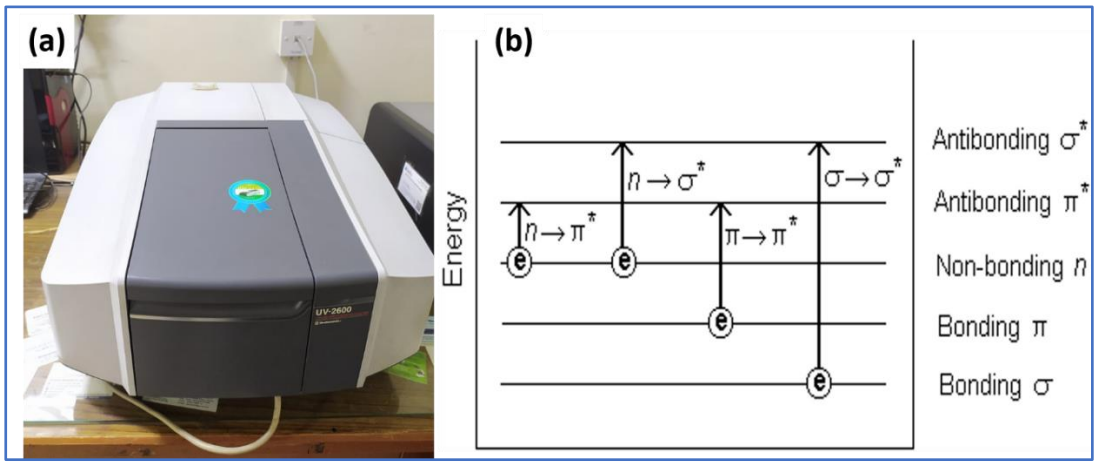

Figure 2.8 (a) Photograph of UV-Vis Spectrophotometer (Courtesy: SMST IIT (BHU)) (b) Schematic of UV-Vis electronic transition concept (Courtesy: Sheffield Hallam University)..

2.2.1.5 Scanning Electron Microscopy (SEM)

SEM is a type of electron microscope that uses a high-energy electron beam to scan the material and produce images of it. It is primarily used to observe material morphology or electrode topography. High energy electron beam strikes through the atom in the sample and produces a Secondary signal electron, a backscattered electron that contains information about the sample surface topography and composition information. An electron gun (containing filament W, Field emission, and Cold Field emission) in a scanning electron microscope creates electrons, which are then accelerated to energies between 1 and 30 keV. Electromagnetic lenses and apertures focus the electron beam and control its diameter. The experiment is conducted with the microscope held in a vacuum (Gun chamber 10^{-6} to 10^{-8} Pa, column Pressure 10^{-4} Pa, and sample chamber 10^{-3} Pa). The electron beam is moved over the specimen surface along the x- or y-axis using scanning coils. As a result of the incident electron beam's interaction with the sample, several signals are produced, detected, processed, and turned into images or spectra. (figure 2.10(b)). Different interactions may take place as an electron beam bombards the specimen surface (figure 2.9). The electron may change direction and lose a small amount of energy (1 eV) as a result of being scattered by atomic nuclei. Backscattered electron refers to the electron that was deflected back by the specimen (BSE). The ratio of backscattered electrons to the scattering element’s atomic number is constant. The incident electrons may interact with the specimen electrons inelastically, which could cause the emission of secondary electrons with low energy (50 eV) (SE). A characteristic energy X-ray is released if an electron fills the hole left by the secondary electron's higher-energy emission. Other types of emissions, including Auger electrons and cathodoluminescence, may result from the interaction of the

electron beam and the material in addition to the BSE and SE that are utilized to create a picture(Ul-Hamid, 2018). Elemental analysis is done by the EDS (Pegasus EDS, EBSD with octane plus and Hikari Pro) system attached to the SEM. All experimental SEM imaging is done on Carl Zeiss and Nova Nano SEM 450

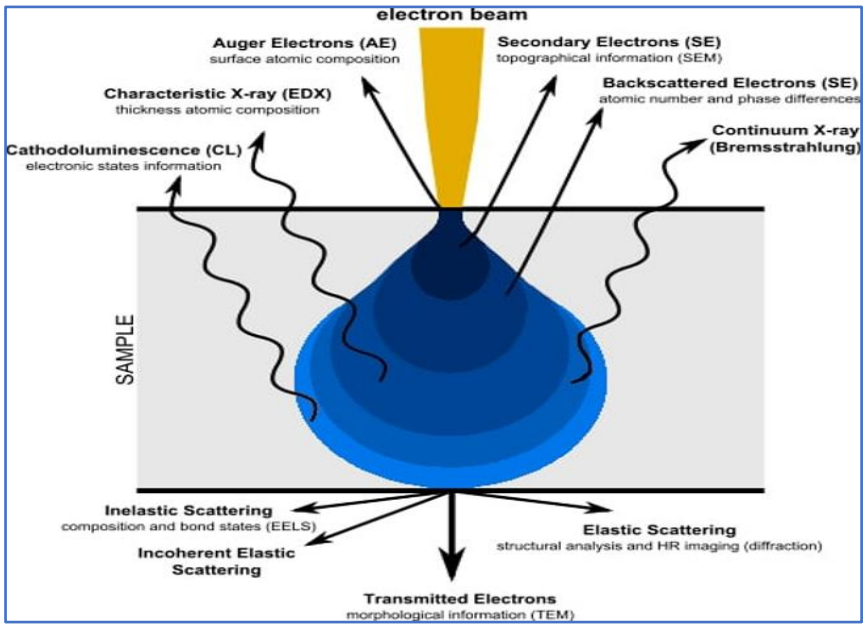

Figure 2.9 Schematic of signal emission from electron bombardment on the sample (Courtesy: Research gate) in SEM.

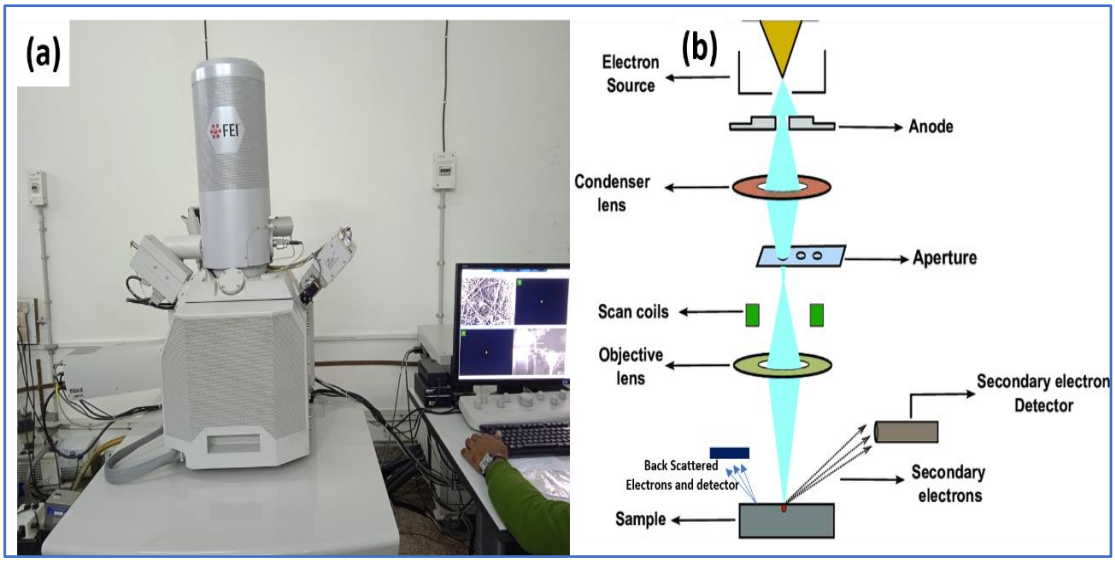

Figure 2.10 (a) Photograph of SEM instrument (Courtesy: CIF IIT(BHU)) (b) Schematic of working mechanism of SEM (Courtesy: Research Gate)

2.2.1.6 Thermogravimetric Analysis (TGA)

TGA is a thermal analysis technique that monitors how much a sample's mass changes as its temperature rises. In a furnace, the sample to be examined is put, and the mass change is calculated as a function of either time (with constant temperature) or temperature (with constant heating rate). As shown in figure 2.11(b), the thermogravimetric apparatus includes a furnace, microbalance, recorder, and temperature programmer. Heating elements are located on the sides of the cylindrical shape of the furnace. The sample is positioned in the furnace's center and is suspended from the microbalance by a tiny wire. The microbalance can measure mass changes of less than 1 microgram in the sample during heating and cooling. The sample is said to be thermally stable in that temperature range if the mass of the sample stays constant over that range of temperatures. TGA also aids in determining the sample's calcination temperature because it provides the maximum temperature at which the sample begins to degrade. An instrument used for TGA analysis is Model TGA 50, Shimadzu (figure 2.11(a))

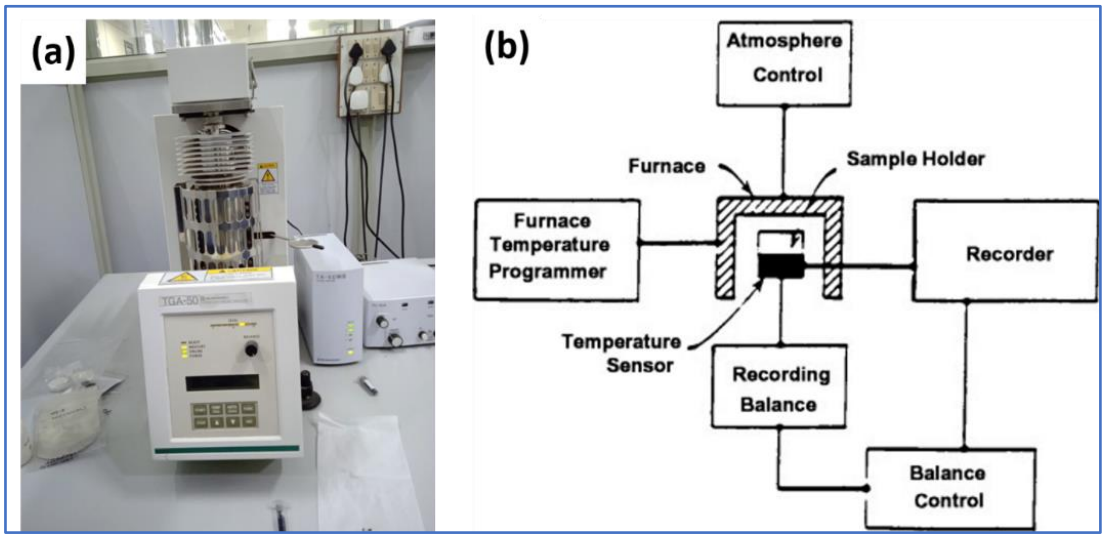

Figure 2.11 (a) Photograph of TGA instrument (Courtesy: IIT(BHU)) (b) Schematic of working of TGA (Courtesy: Science Direct)

2.2.2 Electrochemical characterization

2.2.2.1 Cyclic Voltammetry (CV)

In order to get qualitative and quantitative data about the redox processes taking place inside an electrochemical cell, cyclic voltammetry (CV) scans the potential at an applied sweep rate (often measured in mV/s) and records the resulting current. Two electrode cell is used working and counter electrode (counter is short with the reference electrode), and current is measured between these two. An electrochemical study is carried out on Biologic BT Lab 810. In CV, a current is measured against the Working electrode, and each peak corresponds to the redox process. Signs of current determine the oxidation (positive) and reduction (negative) processes. Peak intensity and area tell us about the number of electron transfers during the electrochemical reaction. Dis-similarity in the peak intensity in the oxidation and reduction arises due to the thermodynamic and kinetic factors that induce overpotential and hysteresis [100]. However, there is some factor that causes the irreversible process, like SEI (solid electrolyte interphase) formation, in which the first cycle form and disappear after the first cycle. It can also modify the WE and raise the difference in the peak intensity and position difference in the first and later CV cycles.

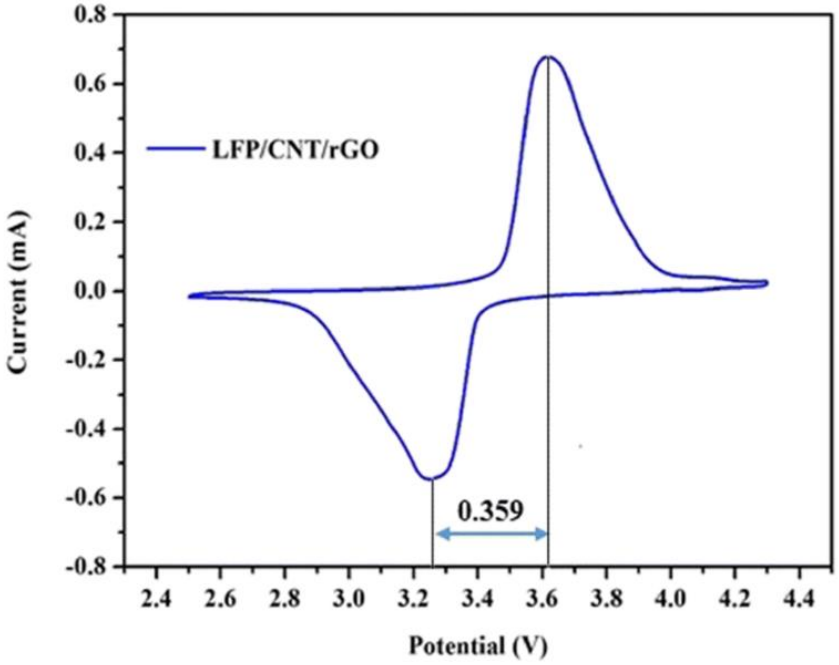

Figure 2.12 Typical CV plot for battery cathode(X. Zhang et al., 2020).

2.2.2.2 Galvanostatic Charge Discharge (GCD)

Galvanostatic charge-discharge or Chrono potentiometry is a method to check the battery performance by applying a steady current *I* to the WE while observing how its potential changes over time. Charge-discharge capacity (*C*) is the total charge in each process, and specific capacity (C_{sp}) is reported in capacity per gram as $C_{sp} = (I \times t) / g$. The equation determines the theoretical specific capacity (*C*) of the electrode material

$$C_{th} = nF/Mw \qquad \text{(Eq. 2.9)}$$

which is the amount of charge involved in the electrochemical reaction per unit mass of the active material, where n is the number of electrons transported per mole of reaction, *M* is the molar mass of the active material, and *F* is the charge of one mole of electrons, or Faraday's constant. The cell's specific capacity is expressed in terms of $mAh.g^{-1}$. The number of hours at which the material becomes fully charged or

discharged is denoted by the symbol C/h, which is also used to describe the galvanostatic cycling rate. For instance, rate C/20 designates the addition or removal of one mole of sodium ion for every mole of active substance every 20 hours. A capacity plot vs. cycle number is a common visual representation of cycling stability. Specific energy retention, as opposed to capacity retention, is a more suitable metric for the cycling inquiry when the cell voltage fluctuates. The electrochemical response of the electrode upon insertion/de-insertion of Na ion for battery applications can be evaluated using this technique(Saba & Jawaid, 2018). Long-term battery performance is evaluated by applying positive and negative currents over a larger number of times within the threshold potential limit. Kinetics study evaluated by applying different currents to an electrode. Slower kinetics results in a larger decrease of capacity with increasing applied current. Differences in the coulombic efficiency by the ratio between the capacities observed for oxidation and reduction can provide additional information about the presence of any irreversible additional redox process(es), such as electrolyte decomposition or SEI formation. The Coulombic efficiency deviation from 100% indicates the occurrence of undesirable reactions in the cell that lead to capacity loss.

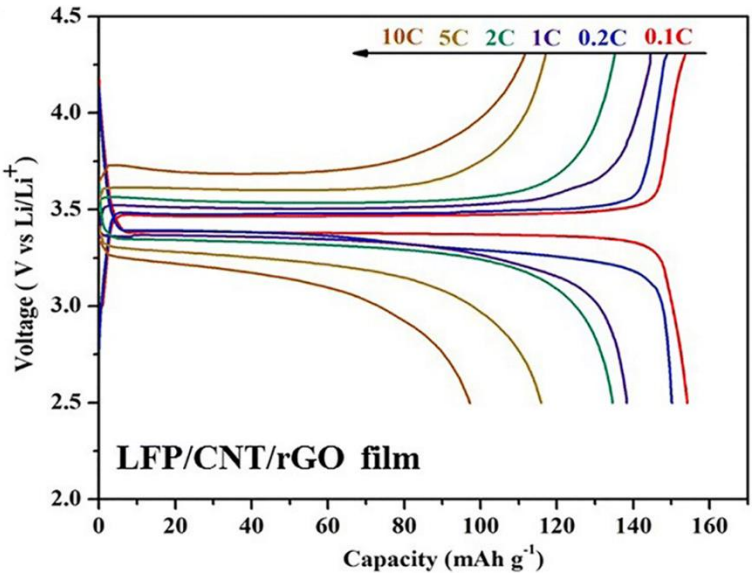

Figure 2.13 Typical Charge discharge plot for battery (X. Zhang et al., 2020).

2.2.2.3 Galvanostatic Intermittent Titration Technique (GITT)

The system is typically out of equilibrium when cycling a cell in a galvanostatic charge-discharge mode; as a result, the experimental potential differs from the theoretical potential. The charge/discharge rate frequently affects this polarization. The system must be kept in an open circuit for a considerable time to reach the potential at thermodynamic equilibrium. The idea behind these GITT measurements is to alternate longer phases of open circuit voltage relaxation (no current) with shorter periods of galvanostatic charge/discharge in order to produce a curve whose values at the conclusion of the open circuit periods are near the thermodynamic potential(Fuentes et al., n.d.; Nickol et al., 2020; Park et al., 2021). With a current rate of C/10 for charging and C/20 for discharging, GITT tests have been carried out for this research at room temperature. 30 minutes of the present pulse are followed by a 120-minute rest period.

2.2.2.3 Electrochemical Impedance Spectroscopy (EIS)

EIS is a crucial method for determining the kinetic parameters of the electrode process, such as the electrolyte, a passivation layer, and the diffusion of lithium and sodium ions. It can determine a cell's ohmic and charge transfer resistance (R_{ct}). A cell's impedance spectrum typically has a semicircle at high frequency and a linear tail at low frequency. The semicircle is attributed to reflecting the kinetic processes like charge transfer resistance or speed of electrochemical reaction; a large value of R_{ct} indicates the slow electrochemical reaction. The linear tail inclined at 45^{o} at low frequency, called Warburg impedance, relates to the diffusion of alkali ions into the bulk of the electrode materials from the

electrolyte. Moreover, EIS can measure the alkali ion (Li+, Na+) diffusion and apparent energy activation of the electrode. Impedance was recorded in the frequency range of 0.01 Hz to 100000 Hz. The ionic conductivity is measured as following

$$\sigma = \frac{l}{R\,A} \qquad \text{(Eq. 2.11)}$$

where σ is the ionic conductivity of the sample, A is the geometrical electrode surface area, R is the solution resistance, l is the electrode thickness. At lower frequencies, Warburg diffusion region diffusion (D) can be calculated as follows(C. Gao et al., 2018; C. Hong et al., 2020)

$$D = \frac{R^2\ T^2}{2(n^2\ F^2\ )^2\ A^2\ C^2\ \sigma w^2} \qquad \text{(Eq. 2.12)}$$

Where R is gas constant (8.314 J mol^{-1} K^{-1}), T is the temperature in kelvin (300 K), n is the number of electron transfers during the redox process, F is Faraday constant (96485 C mol^{-1}), A is the electrode surface area, C is sodium-ion concentration in the electrolyte (1 M), σ_w (Warburg coefficient) is the slope obtained from linear fitting of Z' (real part of impedance) and $\omega^{-0.5}$ (angular frequency) from

$$Z' = R_S + R_{ct} + \sigma_w\,\omega^{-0.5} \qquad \text{(Eq. 2.13)}$$

Where R_s is electrolyte resistance, R_{ct} is charge transfer resistance